

Four-Electron Oxygen Reduction by Brominated Cobalt Corrole

Alex Schechter,^{*,†} Maria Stanevsky,[†] Atif Mahammed,[‡] and Zeev Gross^{*,‡}[†]Department of Biological Chemistry, Ariel University Center of Samaria, Ariel 40700, Israel[‡]Schulich Faculty of Chemistry, Technion-Israel Institute of Technology, Haifa 32000, Israel

Supporting Information

ABSTRACT: The carbon-supported cobalt(III) complex of β -pyrrole-brominated 5,10,15-tris(pentafluorophenyl)-corrole [Co(tpfc)Br₈/C] is introduced as a nonplatinum alternative for electrocatalytic oxygen reduction in aqueous solutions. Through systematic work, the basic kinetic parameters of this reaction were studied, using rotating ring disk electrode electrochemical methods in the pH range of 0–11. Pronounced catalytic activity was detected in acid solutions along with shifts of the Co^{II}/Co^{III} and O₂ redox couples to more positive values (onset of 0.56 V at pH 0). A series of independent measurements have been used to prove that the dominant mechanism for oxygen reduction by Co(tpfc)Br₈/C catalysis is the direct four-electron pathway to water.

Oxygen reduction reaction (ORR) is one of the most important reactions in energy conversion technology, such as fuel cells¹ and metal–air batteries,² as well as in biological energy conversion devices³ and O₂ sensors.^{4,5} Platinum and its alloys are still considered the most active catalysts in an acid medium, but serious concerns are raised regarding the feasibility and availability of platinum for large-scale production of these energy devices. The consequential quest for low-cost alternatives to platinum catalysts has led to an extensive research of macrocyclic transition-metal complexes in the last few decades.^{6,17} ORR aided by phthalocyanine- and porphyrin-based catalysts has been extensively studied,^{8,9} but much less is known about the utility of metal corroles regarding heterogeneous O₂ reduction.^{10–13} Prominent 4e[−] reduction to water was only achieved by the binuclear porphyrin-corrole Co₂(PCY) and biscorrole Co₂(BCY) Co complexes, immobilized on graphite electrode and at pH 0.¹⁰ ORR catalysis by the mononuclear corroles Co(Me₄Ph₅Cor) (pH 0)¹⁰ and Co(mapc-t) (pH 4–11) promotes mainly H₂O₂ production.¹³ The electrochemical O₂ reduction (pH 0, regular and Hangman corroles supported on multiwall carbon nanotubes) could be modulated by proton transfer from the hanging group to the M–O₂ active site as to reduce the % H₂O₂ fraction by 25%.¹² The effective number of electrons in this reaction was below 3, yet the reported % H₂O₂ in this work is among the lowest reported for mononuclear corroles.

Our approach was to synthesize and measure the catalytic activity and ORR properties on the cobalt(III) complex of β -pyrrole-brominated 5,10,15-tris(pentafluorophenyl)corrole [Co(tpfc)Br₈; Figure 1a]. This structure contains the highest possible number of electron-withdrawing groups on a corrole ring, and we expected this to shift Co^{II/III} and Co^{III/IV} to much

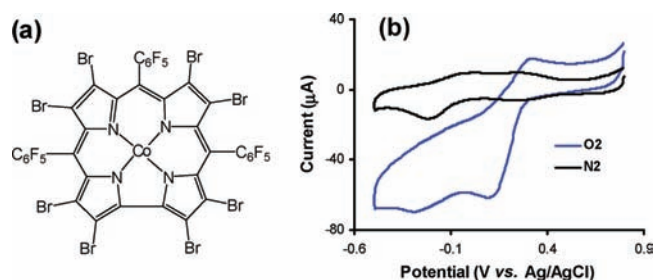


Figure 1. (a) Chemical structure of Co(tpfc)Br₈. (b) Cyclic voltammetry (50 mV/s) of Co(tpfc)Br₈/C, pH 4 phosphate buffer solution, in N₂- and O₂-saturated solutions.

more positive potentials.^{14–16} We describe here ORR kinetics on our catalyst within a wide range of pHs.

Figure 1b shows the cyclic voltammograms of Co(tpfc)Br₈ supported on the high-surface-area carbon support XC72 [Co(tpfc)Br₈/C] in both N₂- and O₂-saturated aqueous phosphate solutions, at pH 4. There was no evidence for O₂ reduction by the catalyst-free carbon support, but Co(tpfc)Br₈/C displayed an ORR onset potential of 0.32 V with peaks at +0.11 and −0.29 V (and +0.56, +0.35, and −0.05 V, respectively, at pH 0). The ORR onset potential follows closely that of Co^{III} reduction to Co^{II} under N₂ at low pH values, and the observation of two peaks is consistent with the sensitivity of that redox couple to axial ligands (H₂O and H₂PO₄[−] under current conditions).¹⁰ A comparison with other mononuclear cobalt corroles reveals that the 0.56 V ORR onset potential of Co(tpfc)Br₈/C (pH 0) is the highest on record: 0.43–0.48 V Hangman corroles (pH 0),¹² 0.38 V for Co(Me₄Ph₅Cor)¹⁰ pH 0, and ~0.14 V for Co(mapc-t)¹³ (pH 7).

A systematic study of ORR catalyzed by Co(tpfc)Br₈/C was carried out using a rotating ring disk electrode (RRDE), by applying linear sweep voltammetry (LSV) from +0.78 to −0.3 V or down to −0.5 V at pH ≥ 7. While the disk potential was linearly scanned, the platinum ring potential was set to 0.98 V, which allows for examination of the diffusion-controlled oxidation of H₂O₂ to O₂. This potential is well below the oxidation potential of H₂O and above the reduction potential of O₂ in acidic pH. Figure 2a demonstrates the results of typical O₂ reduction by LSV measured at selected electrode rotation speeds. More current is obtained at higher rpm (rounds per minute), and the shape of each curve starts with a sharp current

Received: October 3, 2011

Published: December 19, 2011

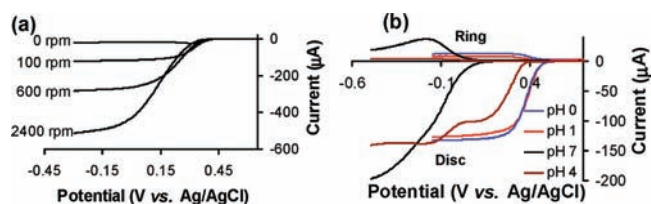
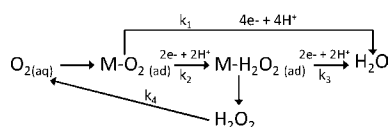


Figure 2. O₂ reduction measurements by LSV of 2 mV/s of Co(tpfc)Br₈/C using (a) a RRDE (0–2400 rpm) in a phosphate buffer at pH 2 and (b) disk (cathodic currents) and platinum ring (poised to 0.98 V; anodic currents) electrodes at 100 rpm in solutions of pH 0, 1, 4, and 7.

increase corresponding to kinetic control reaction or a mixed kinetic and mass-transport rate, followed by a constant limiting current. The limiting current is a typical indication of a fast reaction, hence ascribed to diffusion. At pH above 7, the limiting current is only seen at the lowest applied potential and is not fully established (Figure 2b). The anodic current in Figure 2b shows H₂O₂ oxidation on the RRDE platinum ring, at a fixed rotation speed of 100 rpm and selected pHs. The corresponding H₂O₂ oxidation current on the ring should be correlated with the relevant disk activity. Ring currents were corrected by the collection coefficient factor *N* of the electrode.

ORRs are most frequently characterized by two competing reaction pathways (Scheme 1):¹⁷ (a) 4e[−] reduction directly to

Scheme 1



H₂O (*k*₁); (b) 2e[−] reduction to H₂O₂ (*k*₂), which may be followed by slower reduction to H₂O by the same catalyst (*k*₃). H₂O₂ can detach from the electrode surface and thus be detected by the ring electrode in RRDE experiments (*k*₄).

One distinction between the 4e[−] and 2e[−] pathways is by the ratio of the ring current (*I*_r) to disk current (*I*_d).¹⁷ The RRDE curves presenting *I*_d and the corresponding *I*_r at pH of 0, 1, and 7 are presented in Figure 2b. There is a simultaneous increase in the O₂ reduction peak on the disk and H₂O₂ oxidation on the ring. It is also seen in Figure 2b that H₂O₂ oxidation displays a constant current on the ring (*I*_r) in parallel to a diffusion-limiting current on the disk. This means that the ratio of the ring-to-disk currents (*I*_r/*I*_d) is potential-independent below 0.3 V. Similar behavior is seen at pH 2 and 4 (not shown). At pH 7, where no limiting current is attained, the ring current initially increases and reaches a maximum at −0.2 V and then decreases at even lower potentials. We attribute this change in the ring current as a shift between the 2e[−] mechanism (*k*₂ and *k*₃) and the 4e[−] mechanism (*k*₁) at high overpotentials.¹⁸ Nevertheless, at low pH, the predominant path is 4e[−], as argued below.

The two other complementary parameters that serve well as indicators for the reaction pathway are the number of electrons (*n*) in the overall reaction and the % H₂O₂. These parameters were calculated from eqs 1 and 2 using the RRDE results.¹⁹

$$n = 4I_d / (I_d + I_r/N) \quad (1)$$

$$\%H_2O_2 = 100(2I_r/N) / (I_d + I_r/N) \quad (2)$$

Table 1 summarizes the calculated values of *n* and % H₂O₂ at pH 0–9 and at overpotentials that correspond to both *E*_{1/2} and

Table 1. Total Number of Electrons *n* and % H₂O₂ at Selected pHs

pH	<i>n</i> ^a	% H ₂ O ₂ ^a	<i>n</i> ^b	% H ₂ O ₂ ^b
0	3.6	19.1	3.7	15.2
1	3.8	10.7	3.8	11.1
3	3.8	9.5	3.9	4.6
4	3.9	2.5	4.0	1.0
7 ^c	3.0	49.7	3.7	17.0
9 ^c	3.7	16.8	3.9	7.0

^aMeasured at *E*_{1/2}. ^bMeasured at *I*_L. ^cThe limiting current was not reached.

the final potential, as illustrated in Figure 2b. The number of electrons involved in ORR is somewhat lower at *E*_{1/2} than at the final measured potential but is 3.7–4 at almost all pH values. A reciprocal behavior is seen in the H₂O₂ percentage; higher values of H₂O₂ are observed at *E*_{1/2} than at lower potentials (high overpotentials). Interestingly, the highest *n* values and lowest % H₂O₂ are at the intermediate pH of 3–4. At these pHs, ORR is essentially assigned completely to reduction of O₂ to H₂O via the direct 4e[−] pathway with no peroxide formation. Comparison with previously reported values for mononuclear Co corroles (55% H₂O₂ for Co(Me₄Ph₅Cor),¹⁰ 40% H₂O₂ and *n* = 2.7 at *E*_{1/2} for Co(tpfc)Cl, and 25–55% with *n* = 2.5–2.9 by the Hangman corroles),¹² clearly shows that the bromine-substituted corrole has a much higher selectivity for the desirable 4e[−] reaction.

The ability of Co(tpfc)Br₈/C to reduce the H₂O₂ molecules possibly formed in the 2e[−] ORR path was also examined, by adding 0.25 mM H₂O₂ to a 1 M HClO₄ O₂-free solution and applying LSV to this electrode while revolving at 100 rpm. The measured cathodic current under these conditions was about 2 orders of magnitude lower than that of an O₂-saturated solution. This clearly shows that the catalytic activity of Co(tpfc)Br₈ toward H₂O₂ at pH 0 is actually negligible, consistent with previous reports on both mono- and bis-cobalt corroles.^{10,20} These results suggest that *k*₃ in Scheme 1 equals zero and hence could be fully detected by the ring, unlike H₂O₂ on catalysts like platinum. What is more, when H₂O₂ was added to an O₂-saturated solution, the LSV measured at 300 rpm and pH 0 revealed a negative effect on the ORR reduction current: the measured reduction potential at 0.9 mA decreased from 0.38 to 0.31 V and 0.23 V as the H₂O₂ concentration increased from 0 to 0.01 mM and 0.1 M, respectively.

Resolution of the ORR kinetic current was carried out by analyzing the RDE results by the Koutecky–Levich method.

$$1/I_c = 1/I_k + 1/I_L(1/\omega^{0.5}) \quad (3)$$

Figure 3a show a series of Koutecky–Levich plots (1/cathodic current (1/*I*_c) versus 1/square root of the rotating speed (ω^{−0.5}; eq 3) measured at increasing overpotential (*η*) applied to Co(tpfc)Br₈/C RRDE in a perchloric acid solution of pH 0. The slopes of the lines equal the inverse Levich limiting current (*I*_L^{−1}), and the intercept equals the 1/kinetic current (*I*_k^{−1}) at each potential. *I*_k increases with the applied overpotential, as expected from the Tafel equation of an irreversible electrochemical reaction.²¹ However, in the pH range of 11–4, there was very little change in the kinetic currents, while distinctive increases were seen below pH 4.

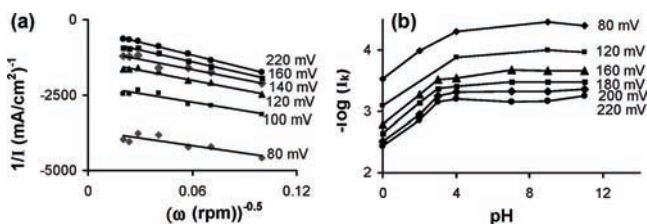


Figure 3. Typical Koutecky–Levich plots of $1/I$ versus $\omega^{-0.5}$ at selected overpotentials at 1 M HClO_4 (a) and the pH dependence of I_k from Koutecky–Levich plots at pH 0–11 and overpotentials of 80–220 mV (b).

Figure 3b shows the pH dependence of the ORR kinetic current presented in a logarithmic scale. The slope at $\text{pH} < 4$, which corresponds to the order of the reaction in $[\text{H}^+]$ $[\rho(\text{H}^+)]$, is derived from $(-\partial \log I_k / \partial \text{pH})_{E, [\text{O}_2]}$, to yield a slope of 0.25 on average. This value is much smaller than 1.0 reported for phthalocyanines absorbed on graphite electrodes,²² as well as the data for $\text{Co}(\text{mapc-t})$, from which $\rho(\text{H}^+)$ can be calculated as 0.5–1 at pH 4–11.¹³ The much lower values of $\rho(\text{H}^+)$ in our study imply that the first electron transfer accompanied by O_2 adsorption, and not proton transfer, is the rate-limiting step in the case of $\text{Co}(\text{tpfc})\text{Br}_8/\text{C}$.^{1,23,22}

The calculated Tafel slopes ($\partial \eta / \partial \log I_k$) measured at the pH range of 11–0 increased from about 110 mV/decade at pH 11 to 146 mV/decade at pH 0. These relatively high Tafel slope values provide further evidence that a first one-electron transfer step is the rate-determining step at those potentials assuming a transfer coefficient of $\alpha = 0.5$.^{23,24}

The close proximity of the $\text{Co}^{\text{III/II}}$ redox potential under N_2 to that measured at half of the limiting current in the LSV–RDE experiment under O_2 and pH 0–4, is an excellent example of the redox activation of the catalyst. At higher pH the reaction is more sluggish (Figure 3b), and the redox resides at higher potentials than $E_{1/2}$. We ascribe this behavior to axial ligand effects, which interferes with O_2 adsorption at pH 4–11. Below pH 4, the affinity to axial ligands is heavily reduced because of their protonation, which is consistent with the pH dependence of the $\text{Co}^{\text{III/II}}$ peak potential (gradually decreasing from 0.4 V at pH 0 to 0.22 V at pH 4, with no further changes at higher pHs).

The heterogeneous rate constant k^0 was calculated for each of the kinetic currents at pH 0. As the overpotential increased toward cathodic potentials, the ORR reaction rate constant increased as well: from $9 \times 10^3 \text{ M}^{-1} \text{ s}^{-1}$ at 0.1 V to $6.6 \times 10^4 \text{ M}^{-1} \text{ s}^{-1}$ at an overpotential of 0.22 V. Collman reported a value of $4 \times 10^3 \text{ M}^{-1} \text{ s}^{-1}$ at 0.2 V for $\text{Fe}(\text{tpfc})$, which corresponds to an overpotential of 0.29 V. The k^0 value calculated in our case is more than 1 order of magnitude higher, in support of faster kinetics. Kadish reported a k^0 value of $5.7 \times 10^5 \text{ M}^{-1} \text{ s}^{-1}$ for ORR on $\text{Co}(\text{Me}_4\text{Ph}_5\text{Cor})$ at an arbitrary potential.¹⁰

We have introduced the cobalt(III) complex of a β -pyrrole-brominated corrole as the catalyst for molecular O_2 reduction at a very positive potential, made possible because of the effect of the electron-withdrawing bromides on the $\text{Co}^{\text{III/II}}$ redox potential. The carbon-supported catalyst exhibits very fast reduction kinetics at $\text{pH} \leq 4$, and the vast majority of the O_2 electroreduction proceeds directly to H_2O . Both the pH-dependent kinetic currents and the Tafel slopes indicate that the rate-limiting step is O_2 adsorption to the catalyst's active site. A comparison with other corrole-based ORR catalysts reveals the superiority of $\text{Co}(\text{tpfc})\text{Br}_8$ by all of the above-listed parameters. Taken together with the recently reported

efficiency of electron-poor cobalt(III) corroles as catalysts for an O_2 -evolving reaction (the reverse of ORR),²⁵ suggests a great potential of these complexes in fuel cells.

■ ASSOCIATED CONTENT

Supporting Information

Full experimental details. This material is available free of charge via the Internet at <http://pubs.acs.org>.

■ AUTHOR INFORMATION

Corresponding Author

*E-mail: salex@ariel.ac.il (A.S.), chr10zg@tx.technion.ac.il (Z.G.).

■ ACKNOWLEDGMENTS

Support by Nevet grant - GTEP - RBNI is acknowledged.

■ REFERENCES

- Zhang, J. *PEM fuel cell electrocatalysts and catalyst layers: fundamentals and applications*; Springer: London, 2008.
- Girishkumar, G.; McCloskey, B.; Luntz, A. C.; Swanson, S.; Wilcke, W. *J. Phys. Chem. Lett.* **2010**, *1*, 2193.
- Logan, B. E. *Microbial fuel cells*; Wiley-Interscience: Hoboken, NJ, 2008.
- O'Hare, D.; Winlove, C. P.; Parker, K. H. *J. Biomed. Eng.* **1991**, *13*, 304.
- Wang, B. *J. Power Sources* **2005**, *152*, 1.
- Yeager, E. *J. Mol. Catal.* **1986**, *38*, 5.
- Jahnke, H.; Schonborn, M.; Zimmermann, G. *Top. Curr. Chem.* **1976**, *61*, 133.
- Kiros, Y. *Int. J. Electrochem. Sci.* **2007**, *2*, 285.
- Zagal, J.; Páez, M.; Tanaka, A. A.; dos Santos, J. R. Jr.; Linkous, C. A. *J. Electroanal. Chem.* **1992**, *339*, 13.
- (a) Kadish, K. M.; Fremont, L.; Ou, Z.; Shao, J.; Shi, C.; Anson, F. C.; Burdet, F.; Gros, C. P.; Barbe, J. M.; Guillard, R. *J. Am. Chem. Soc.* **2005**, *127*, 5625. (b) Mahammed, A.; Giladi, I.; Goldberg, I.; Gross, Z. *Chem.—Eur. J.* **2001**, *7*, 4259.
- Marom, N.; Kronik, L. *Appl. Phys. A: Mater. Sci. Process.* **2009**, *95*, 159.
- Dogutan, D. K.; Stoian, S. A.; McGuire, R. Jr.; Schwalbe, M.; Teets, T. S.; Nocera, D. G. *J. Am. Chem. Soc.* **2010**, *133*, 131.
- Collman, J. P.; Kaplun, M.; Decreau, R. A. *Dalton Trans.* **2006**, 554.
- Palmer, J. H.; Day, M. W.; Wilson, A. D.; Henling, L. M.; Gross, Z.; Gray, H. B. *J. Am. Chem. Soc.* **2008**, *130*, 7786.
- Golubkov, G.; Bendix, J.; Gray, H. B.; Mahammed, A.; Goldberg, I.; DiBilio, A. J.; Gross, Z. *Angew. Chem., Int. Ed.* **2001**, *40*, 2132.
- Mahammed, A.; Tumanskii, B.; Gross, Z. *J. Porphyrins Phthalocyanines* **2011**, *15*, 000.
- Wroblowa, H. S.; Yen Chi, P.; Razumney, G. *J. Electroanal. Chem.* **1976**, *69*, 195.
- Chang, C.-C.; Wen, T.-C. *Electrochim. Acta* **2006**, *52*, 623.
- Lefèvre, M.; Dodelet, J.-P. *Electrochim. Acta* **2003**, *48*, 2749.
- Liu, H. Y.; Abdalmuhdi, I.; Chang, C. K.; Anson, F. C. *J. Phys. Chem.* **1985**, *89*, 665.
- Bard, A. J.; Faulkner, L. R. *Electrochemical methods: fundamentals and applications*; Wiley: New York, 1980.
- Zagal, J.; Bindra, P.; Yeager, E. *J. Electrochem. Soc.* **1980**, *127*, 1506.
- Tarasevich, M. R.; Radiyschikina, K. A.; Androuseva, S. I. *Bioelectrochem. Bioenerg.* **1977**, *4*, 18.
- Gileadi, E. *Electrode kinetics for chemists, chemical engineers, and materials scientists*; VCH: New York, 1993.
- Dogutan, D. K.; McGuire, R. Jr.; Nocera, D. G. *J. Am. Chem. Soc.* **2011**, *133*, 9178.